AIAA JOURNAL
Vol. 39, No. 8, August 2001

Megahertz Visualization of Compression-Corner Shock Structures

Pingfan P. Wu* and Richard B. Miles†
Princeton University, Princeton, New Jersey 08544

The interactions between shock waves and turbulent boundary layers in a Mach 2.5 wind tunnel have been visualized by a megahertz-rate imaging system. The shock waves were produced by two-dimensional compression corners having angles of 14 and 24 deg, and the flows were, respectively, attached and separated. At the compression corner, the sequential images clearly indicate the correlation between the shock motion and the incoming turbulent boundary layer. Some large eddies in the boundary layer cause the shock to move in the streamwise direction for distances as large as the boundary-layer thickness at a frequency as high as large-eddy frequency (U_e/δ), but other eddies seem to have minor effect on the shock wave. The images also indicate how the shock waves influence the boundary-layer structures.

I. Introduction

THE shock-wave/boundary-layer interaction (SWBLI) is a very important supersonic flow phenomenon that can cause changes in heat transfer, flow separation, amplification of turbulence, generation of strong secondary flows, and unsteadiness.[1] Although the SWBLI in the laminar flow has been studied in detail and is now fairly well understood,[2] the more complex interactions between shock waves and turbulent boundary layers continue to be of great interest. Because of the high Reynolds numbers encountered in most practical applications, direct numerical simulation is unrealistic for the calculation of turbulent flow interaction.[1] Reynolds-averaged Navier–Stokes models are generally inaccurate for prediction of critical engineering data in the flow interactions, such as rms fluctuation pressure and heat surface transfer.[3] Alternatively, large-eddy simulation[4] is a more promising technique for the computation of shock-wave and turbulent boundary-layer interactions.[5] At present, experiments are required to provide the physical picture. All of the computational approaches need to be validated against experimental measurements.

The two-dimensional compression ramp flows have been extensively studied[1,6] because this is the simplest model in generating the SWBLI and most of the generic effects of compressibility in two-dimensional interactions can be understood from an examination of the compression-corner flows.[1] Experiments have shown that the shock is unsteady in the presence of a turbulent boundary layer.[6] Through work of the past 25 years, it has been recognized that the incoming turbulent boundary drives the shock motion.[5–9] However, the characteristics of the boundary-layer and shock-wave coupling are still not clear, particularly in regard to the following questions:

1) What is the scale of the shock motion? Is it just small-scale jitter, or large-scale fluctuation?

2) What features of the boundary-layer structures drive the shock motion?

3) How does the shock wave influence the boundary layer?

The major limitation on previous experiments is the instrumentation. Most of the work aimed at investigating unsteadiness in the shock wave has relied on the measurements by pressure transducers along the wall. In the spatial domain, the pressure transducers only yield a point measurement at the wall. They give no information about the flowfield. In the frequency domain, the fastest frequency response among these transducers is only 50 kHz (Refs. 6 and 7). Cogne et al.[10] and then Beresh et al.[11] and Poggie and Smits[12] have used double-pulse planar laser imaging to visualize the interaction between the shock wave and boundary layer. Particle imaging velocimetry has also been used to interpret the separation shock and flow motion by Beresh et al.[13] Their planar images give enough resolution to visualize the large-eddy structure, but two sequential images are not enough to show the shock evolution.

It has been suspected that the large eddies in the boundary layer interact directly with the shock.[5,6,8] In Cantwell's review paper,[14] data show that the physical dimensions of the large eddies are on the order of the boundary-layer thickness δ. The data also show that the convection velocity U_c of the large eddies is on the same order of the freestream flow velocity U_e (more specifically, is $0.6–0.9U_e$). The large eddy frequency U_e/δ of the supersonic flow in the wind-tunnel facilities that we are using is above 100 kHz. Thus, it can be assumed that important phenomena associated with the SWBLI interaction may occur at or above 100 kHz.

In this paper, the unsteady shock structure was visualized by a megahertz-rate imaging system. The megahertz-rate imaging system[15] can capture 30 sequential images at framing rates as short as one image per microsecond. These image sequences illustrate the dynamics of the SWBLI process. The interactions in a Mach 2.5 wind tunnel were produced by two-dimensional compression corners having angles of 14 and 24 deg, and the flows were attached and separated from the tip of the wedge, respectively.

II. Facilities

The megahertz-rate imaging system consists of a pulse-burst laser and a charge-coupled device (CCD) framing camera.[15] The megahertz repetition rate pulse-burst laser system can generate more than 30 pulses at each burst. The pulses repeat at up to 1 MHz, and the bursts repeat at 9 Hz. The time duration of each pulse is variable, and for this work was set to about 10 ns. The average pulse energy is 100 mJ at 1.06 μm and 25 mJ at 0.532 μm. The linewidth of the laser pulse (~90 MHz) is close to the Fourier transform limit, so that it is suitable to be used in the techniques that require narrow linewidth, such as the filtered Rayleigh scattering (FRS).[16] The megahertz framing rate CCD camera is built by Princeton Scientific Instruments, Inc. It uses on-chip storage technique and can store 30 frames. Details about the megahertz-rate laser and camera technology may be found in Ref. 15.

The Mach 2.5 wind tunnel was built by Smith.[17] It has a test section of 13×26 mm. The test section is 16 in. (406 mm) downstream of the throat, and so the incoming boundary layer undergoes natural transition well upstream of the test section. All of the four sides of the test section are made of glass windows to provide optical access. The stagnation temperate T_0 is 258 K (Ref. 17) and stagnation pressure P_0 is 120 psig (0.83 MPa). The Reynolds number based on the momentum thickness is approximately 1.4×10^4 (Ref. 17).

Presented as Paper 2000-0647 at the AIAA 38th Aerospace Science Meeting, Reno, NV, 10–13 January 2000; received 5 June 2000; revision received 5 January 2001; accepted for publication 1 February 2001.

*Graduate Student, Department of Mechanical and Aerospace Engineering. Member AIAA.

†Professor, Department of Mechanical and Aerospace Engineering. Fellow AIAA.

At the test section, the boundary layer thickness δ is approximately 3.3 mm. The large-eddy frequency U_e/δ is around 150 kHz.

To enhance the Rayleigh scattering signal, gaseous CO_2 was seeded into the flow well upstream of the plenum chamber at a level less than 1% (weight). After the nozzle, due to the temperature drop of the supersonic flow, CO_2 condensed to fine clusters of which the average radius was estimated less than 10 nm (Ref. 18). In the warmer thermal boundary layer, the CO_2 cluster sublimated. In the Rayleigh scattering, the particle scattering cross section scales as the particle radius to the sixth power. The seeding resulted in very high imaging contrast with the mainstream flow producing bright scattering and very little scattering from the boundary layer. This contrast was used to reveal the organized boundary-layer structures. Nau[19] and Smith[17] have correlated the mass flux signal measured by the hot-wire probe and the simultaneous scattering from the condensed clusters. They found that the intensity fluctuation profile of the Rayleigh scattering from the condensed clusters can approximately represent the density fluctuation in the outer part of boundary layer, $y/\delta > 0.6$.

Two brass wedges, with 14- and 24-deg angles, respectively, have been used to generate the shock waves in the tunnel. Each of the two wedges is 2 in. (50.8 mm) long by 1 in. (25.4 mm) wide by 0.085 in. (2.2 mm) thick and fastened to one side of the wind tunnel. To have the streamwise view, a 0.031-in.- (0.8-mm-) wide slit was cut in the center of the wedge to let the laser sheet pass through. The size of the slit is hundreds of times larger than the viscous length ν/U_τ and might be expected to introduce errors at the small scales. However, because we are primarily interested in the unsteadiness of the shock system associated with the large-scale motion, for which the characteristic length δ is more than three times larger than the slit size, the influence of the slit on the overall dynamics process may be acceptable.

III. Experiment

Figure 1 shows the experimental setup to obtain the streamwise view of the shock structure. The direction of the flow is from left to right. The second harmonic output of the pulse-burst laser was formed into an approximately 2.5 cm wide by 100 μm thick sheet and directed into the flow at 60 deg with respect to the freestream motion. The 60-deg angle was chosen to generate enough of Doppler frequency shift for the FRS which was used to suppress background scattering and to highlight velocity discontinuities. Only 1 mJ/pulse of laser energy is needed to generate enough scattered signal. The megahertz framing rate CCD camera had its optical axis perpendicular to the plane of laser sheet. In front of the camera, there was a well-characterized iodine cell, an optically thick filter with strong spectral absorption lines. The frequency of the pulse-burst laser was tuned by an IBM personal computer. A small amount of the laser output passed through a high-power reflection mirror and was used for frequency reference and calibration. The transmitted light was split by a 50/50 mirror. One part of the signal was collected by a photodiode (PD2) to monitor the fluctuation in laser output. The other part of the signal passed through an iodine filter and was collected by a second photodiode (PD1) to determine the light attenuation through the iodine cell. As the laser was tuned in frequency, this signal was used to calibrate the laser frequency with respect to the iodine absorption line.

IV. Experimental Results

A. 14-Degree Wedge

Figure 2a shows a typical sequence of six streamwise view images of the boundary layer over the 14-deg wedge. The image size is 0.5×0.5 in. (12.7 mm), the frame rate is 500 kHz, and the time interval between frames is 2 μs. The bright straight line at the right bottom corner is the wedge. The extension of the shock in the outer boundary layer to the wall remains close to the tip of the wedge. The shock wave fluctuates in response to particular incoming turbulent boundary-layer structures. Note that the location of the shock well outside of the boundary layer, $>2\delta$, stays relatively constant. What varies is the curvature of the shock near the outer portion of the boundary layer.

The SWBLI is three dimensional, and so the experiment was also setup to obtain planform-view images. Smith et al.[8] have used the single-shot planform-view Rayleigh scattering to visualize the turbulent SWBLI. In this experiment, we visualized the interaction with the megahertz-rate pulse-burst laser. The layout was similar to that shown in Fig 1, except the laser sheet was parallel to the wall of the wind tunnel and passed over the surface of the wedge. The distance between the laser sheet and the wall was about 3 mm. Figure 2b shows sequential planform images, each separated by 2μs. The shock wave now turns into a wavy line, and the boundary layer structures are seen as dark regions in the flow. A discontinuity in the images can also be seen as the flow crosses the shock. This is because the oblique shock changes the direction of the flow, forcing it out toward the laser sheet plane. From these images, it is particularly apparent that the oscillation of the shock is correlated with the incoming boundary-layer structures. The displacement of the shock wave, which is most apparent in image 4, is about one boundary-layer thickness. The time lapse from frame 1 to frame 4 is only 6 μs, so that this feature develops at a rate close to the large-eddy frequncy, U_e/δ.

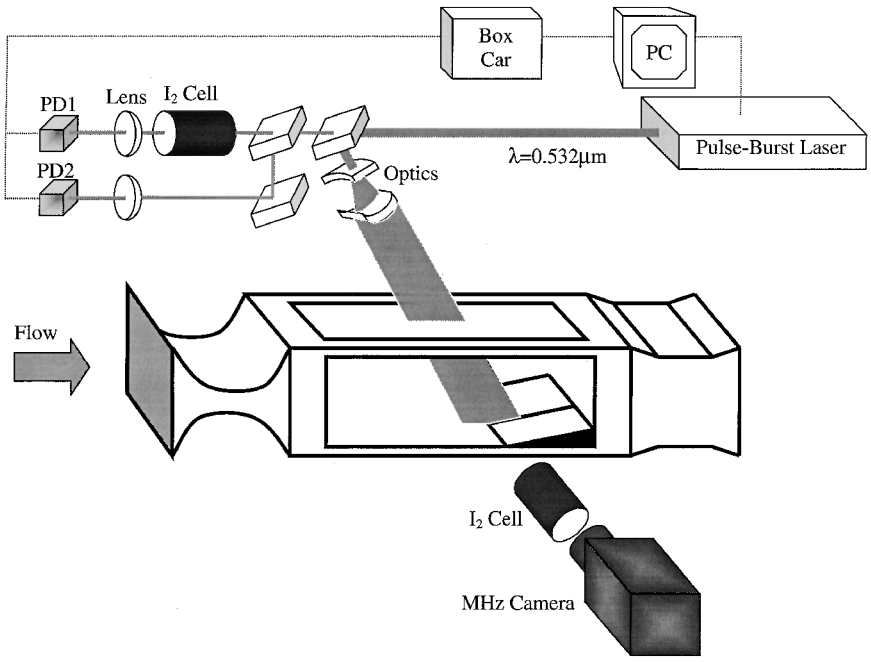

Fig. 1 Experimental setup of SWBLI in Mach 2.5 wind tunnel.

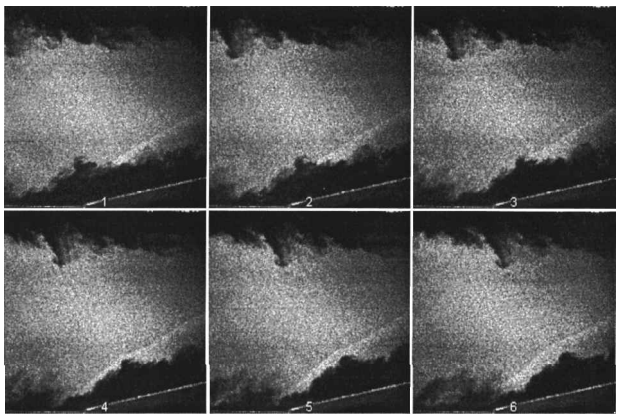

a) Streamwise view

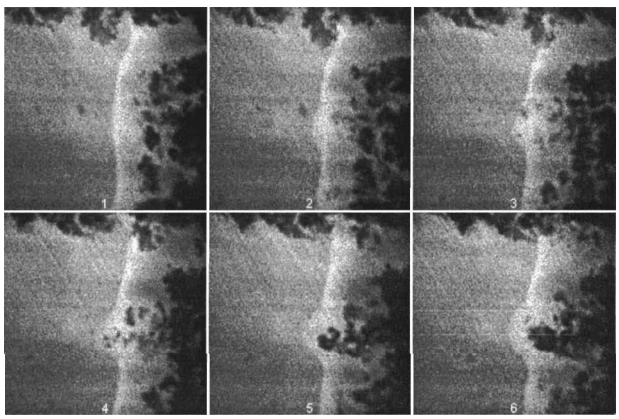

b) Planform view

Fig. 2 Sequential images of Mach 2.5 flow over 14-deg wedge.

B. 24-Degree Wedge

Figure 3 shows sequences of streamwise view images of the boundary layer over a 24-deg wedge with the images size of 0.5×0.5 in. (12.7 mm). The framing rate is again 500 kHz. Because the shock is much stronger than the case of the 14-deg wedge, the flow is separated, and there is a standoff distance between the foot of the shock and the tip of the wedge. The shock is still very sensitive to the incoming boundary-layer structures. The foot of the shock is difficult to see with this technique, but from Fig. 3a, we can see that the shock wave in the center portion of the boundary layer moves parallel to the wall at a distance on the order of δ.

As the flow crosses the shock, its speed decreases, and the scattered light has a small Doppler frequency shift. As the frequency of the pulse-burst laser is tuned, the Doppler shifted scattered signal from different velocity regions is attenuated differently by the spectral filter (iodine cell). With the laser frequency tuned near the center of the iodine absorption, scattering from the low-speed flow and nonmoving elements such as the surface of the wedge is selectively attenuated, as shown in Fig. 4a. Alternatively, as shown in Fig. 4b, the scattering from the high-speed flow can be suppressed. The FRS highlights the structure of shock waves. Where the flow speed changes discontinuously when it crosses the shock, there is a sharp contrast line between the high- and low-speed flow in the images. For some frames (Fig. 4a, frame 6), however, the intensity of the scattering across the shock changes gradually. In this case, not only has the position of the shock moved, but it appears that the structure of the shock has changed from a single shock to an array of compression fans or a group of shocklets.

The image sequences have been formed into loop movies to give a dynamics view of the interaction. The movies may be seen on the Internet at http://www. princeton.edu/~milesgrp/qif/index.html [cited 1 January 2001].

V. Discussion

After analyzing hundreds of sequences of SWBLIs, from both 14 and 24-deg wedges, some common features of the sequences can be found.

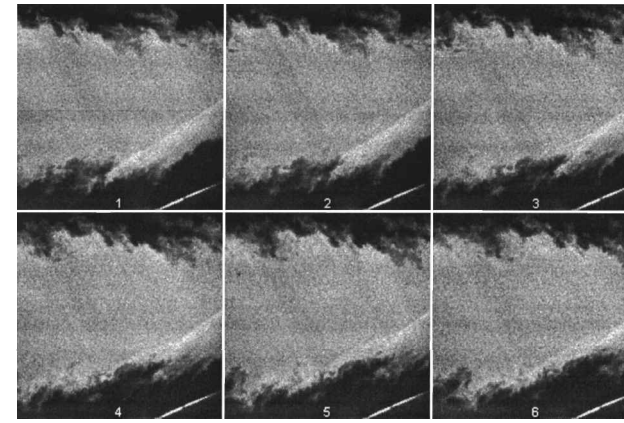

a)

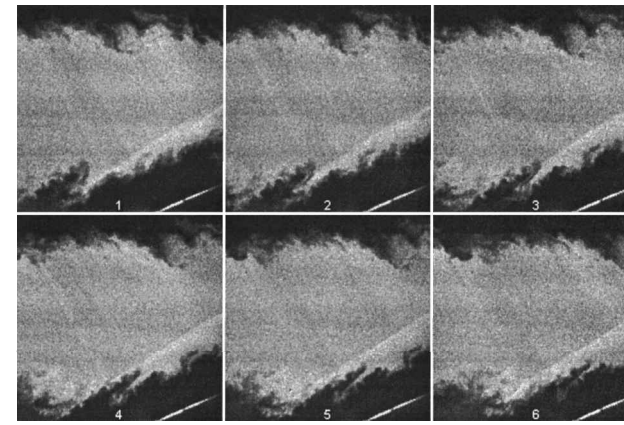

b)

Fig. 3 Sequential streamwise images of Mach 2.5 flow over 24-deg wedge: a) incoming boundary-layer structures have impact on the shock structure, and b) incoming boundary-layer structures have little impact on the shock structure.

After it passes the shock, the overall boundary-layer structure still keeps its identity, except that the shape of the structure is compressed in the direction normal to the shock. A similar result has also been found by Cogne et al.[10] The interaction of the shock wave on the outer boundary layer is close to a rapid distortion process (Ref. 1, Chap. 4.4), which means that the interaction time is much shorter than the turbulent structure energy-containing motions timescale T_t ($T_t = K/\varepsilon$, where k is the mean turbulent kinetic energy and ε is its mean dissipation rate per unit mass). Thus, the eddies still keep their identities after the shock. Figure 5 is an example of this. In Fig. 5, the frame size is 0.5 in. (12.7 mm), and framing rate is 500 MHz. After a boundary-layer structure passes the shock, its length in the streamwise direction scales in about the same ratio as the speed of the outer layer across the shock. Because the flow density increases after the shock, from the continuity equation, the turbulent vortices are compressed. When the structure passes the shock, the velocity component parallel to the shock remains the same, while the velocity component normal to the shock changes. Thus, the turbulent structure is compressed in the direction normal to the shock.

In the outer boundary layer, the shock fluctuation is correlated with the incoming turbulent boundary-layer structures, regardless of whether the flow is separated by the shock (24-deg wedge) or not (14-deg wedge). A low-speed, hot boundary-layer structure always tends to bend the shock upstream (Figs. 2b and 3a). This observation is in agreement with the work by Dolling.[20] In response to some incoming turbulent structure, the shock waves fluctuate for distances on the order of boundary-layer thickness δ in the streamwise direction at a frequency close to the large-eddy frequency U_e/δ. The fluctuation of the shock in the center portion of the boundary layer appears to be similar for both attached and separated flows. The shock motion driven by the incoming turbulent structures is a large-scale, high-frequency motion. In these cases, not only the position of

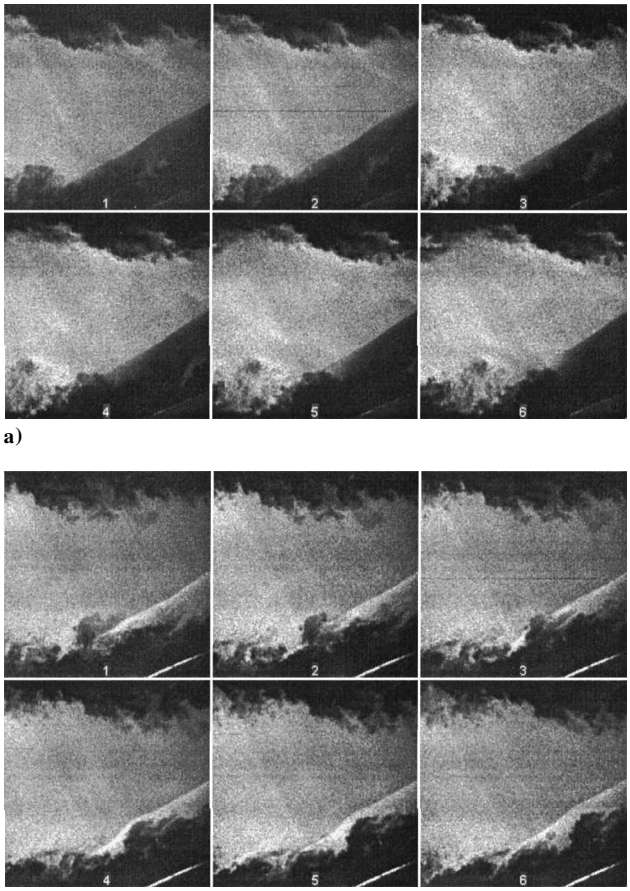

Fig. 4 Filtering used to highlight different speeds of the flow: a) laser frequency tuned so that the filter absorbed low-speed part of the flow and b) laser tuned so that the filter absorbed high-speed part of the flow.

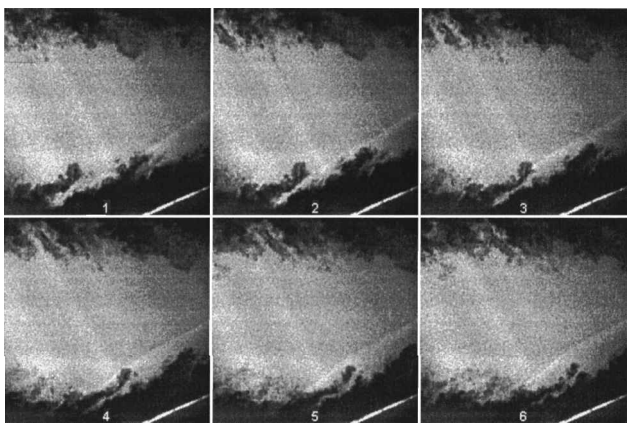

Fig. 5 Sequential streamwise images of Mach 2.5 turbulent boundary-layer structures passing shock wave.

the shock changes, but also the structure of the shock wave changes (Figs. 3a and 4a). The oblique shock caused by a wedge is formed by the coalescence of compression waves that arises in the suppression part of the boundary layer as the flow is turned. The distance above the wall to the point at which a full shock is formed depends on the rate of curvature of this supersonic flow. In the case of flow over 24-deg wedge, a separation bubble is formed in front of the wedge. Like a cavity, the separation bubble oscillates, and the incoming turbulent boundary layer is the driving force. The oscillation of the separation bubble induces its curvature to vary, and so does the shock structure.

The scale of the shock motion also depends on the feature of the incoming boundary-layer structures. The boundary-layer structures oriented normal to the wall (also labeled as hatchback structures)

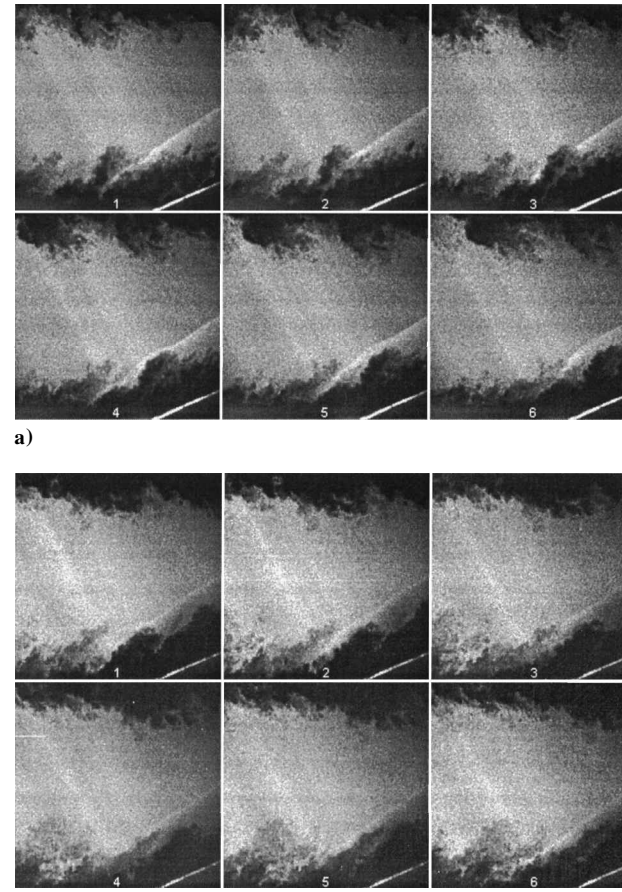

Fig. 6 Comparison of influence on the shock waves by the a) hatchback and b) finger boundary-layer structure.

seem to have the biggest impact on the shock motion (see Figs. 3a, 5, and 6a). However, the shock system seems not to be influenced by the finger shape structures that are inclined about 45 deg in the streamwise direction (see Figs. 3b and 6b). In Fig. 6 the frame size again is 0.5 in. (12.7 mm), and the frame rate is 500 MHz.

VI. Conclusions

The shock structure in a Mach 2.5 wind tunnel has been visualized at a megahertz rate. The shock waves were produced by two-dimensional compression corners having angles of 14 and 24 deg, and the flows were attached and separated from the tip of the wedge, respectively.

The sequential images indicate the interaction between shock waves and incoming turbulent boundary layer.

1) The shock motion is strongly correlated with the incoming turbulent boundary-layer structures. The shock was forced to fluctuate at large-scale (boundary-layer thickness δ) in the streamwise direction and high frequency (U_e/δ, or on the order of hundreds of kilohertz). Not only the position of the shock, but also the character of the shock fluctuates from a single shock to compression fans or groups of shocklets.

2) Different features of the boundary-layer structures have different influence on the shock. The finger structures, which are parallel to the shock, have less influence on the shock than the hatchback structures.

3) Because it is an interaction process, the shock wave also influences the boundary-layer structures. The process of a boundary layer passing a shock wave can be described by the rapid distortion approximation. The boundary-layer structures are compressed, but keep their identities, while the shock was bent by the structures.

One limitation of our seeding technique is that the boundary-layer structures near the hot wall cannot be visualized. We cannot determine whether the shock is attached to the tip of the 14-deg wedge all of the time or not. Experiments incorporating fast pressure sensors at

the wall and wall-seeded flow would be helpful to further the understanding of the separated shock dynamics. It is also recommended to evaluate the flow motion quantitatively through the correlation of the sequential images.

Acknowledgments

This work is supported by Air Force Office of Scientific Research (Grant F49620-97-0373). The authors would also like to acknowledge the helpful discussion with A. J. Smits at Princeton University and W. R. Lempert at Ohio State University.

References

[1]Smits, A. J., and Dussauge, J.-P., *Turbulent Shear Layers in Supersonic Flow*, American Inst. of Physics Press, 1996, Chap. 10, pp. 285.

[2]Adamson, T. C., and Messiter, A. F., "Analysis of Two-Dimensional Interactions Between Shock Waves and Boundary Layers," *Annual Review of Fluid Mechanics*, Vol. 12, 1980, pp. 103–138.

[3]Knight, D. D., "Numerical Simulation of Compressible Turbulent Flows Using the Reynolds–Averaged Naiver–Stokes Equations," *Special Course on Turbulence in Compressible Flows*, R-819, AGARD, 1997.

[4]Reynolds, W. C., "Computation of Turbulent Flows," *Annual Review of Fluid Mechanics*, Vol. 8, 1976, pp. 183–208.

[5]Hunt, D., and Nixon, D., "A Very Large Eddy Simulation of an Unsteady Shock Wave Turbulent Boundary Layer Interaction," AIAA Paper 95-2212, June 1995.

[6]Dolling, D. S., "Unsteady Phenomena in Shock-Wave/Boundary-Layer Interaction," *Special Course on Shock-Wave/Boundary-Layer Interactions in Supersonic and Hypersonic Flows*, R-792, AGARD, 1993.

[7]Erergil, M. E., and Dolling, D. S., "Correlation of Separation Shock Motion with Pressure Fluctuations in the Incoming Boundary Layer," *AIAA Journal*, Vol. 29, No. 11, 1991, pp. 1868–1877.

[8]Smith, D. R., Poggie, J., Konrad, W., and Smits, A. J., "Visualization of the Structure of Shock Wave Turbulent Boundary Layer Interactions using Rayleigh Scattering," AIAA Paper 91-0651, Jan. 1991.

[9]Dolling, D. S., and Murphy, M. T., "Unsteadiness of the Separation Shock Wave Structure in a Supersonic Compression Ramp Flowfield," *AIAA Journal*, Vol. 21, No. 12, 1983, pp. 1628–1634.

[10]Cogne, S., Forkey, J. N., Miles, R. B., and Smits, A. J., "The Evolution of Large-Scale Structures in a Supersonic Turbulent Boundary Layer," *Proceeding of the Symposium on Transition and Turbulent Compressible Flows*, edited by D. E. Stoke, A. J. Smits, and S. A. Sheriff, American Society of Mechanical Engineers, Fairfield, NJ, 1993.

[11]Beresh, S. J., Clemens, N. T., Dolling, D. S., and Comninos, M., "Investigation of the Causes of Large-Scale Unsteadiness of Shock-Induced Separated Flow Using Planar Laser Imaging," AIAA Paper 97-0064, Jan. 1997.

[12]Poggie, J., and Smits, A. J., "Shock Unsteadiness in a Reattaching Shear Layer," AIAA Paper 2000-0140, 2000.

[13]Beresh, S. J., Clemens, N. T., and Dolling, D. S., "The Relationship Between Upstream Turbulent Boundary Layer Velocity Fluctuations and Separation Shock Unsteadiness," AIAA Paper 99-0295, Jan. 1999.

[14]Cantwell, B. J., "Organized Motion in Turbulent Flow," *Annual Review of Fluid Mechanics*, Vol. 13, 1981, pp. 457–515.

[15]Wu, P., Lempert, W. L., and Miles, R. B., "Megahertz Pulse-Burst Laser and Visualization of Shock-Wave/Boundary-Layer Interaction," *AIAA Journal*, Vol. 38, No. 4, 2000, pp. 672–679.

[16]Forkey, J. N., Finkelstein, N. D., Lempert, W. R., and Miles, R. B., "Demonstration and Characterization of Filtered Rayleigh Scattering for Planar Velocity Measurements," *AIAA Journal*, Vol. 34, No. 3, 1996, pp. 442–448.

[17]Smith, M. W., "Flow Visualization in Supersonic Turbulent Boundary Layers," Ph.D. Dissertation, Dept. of Mechanical and Aerospace Engineering, Princeton Univ., Princeton, NJ, June 1989.

[18]Wu, P., "MHz-Rate Pulse-Burst Laser Imaging System: Development and Application in the High-Speed Flow Diagnostics," Ph.D. Dissertation, Dept. of Mechanical and Aerospace Engineering, Princeton Univ., Princeton, NJ, June 2000.

[19]Nau, T., "Rayleigh Scattering as a Quantitative Tool in Compressible Turbulent Boundary Layers," M.S. Thesis, Dept. of Mechanical and Aerospace Engineering, Princeton Univ., Princeton, NJ, June 1995.

[20]Dolling, D. S., "50 Years of Shock Wave/Boundary-Layer Interaction—What Next?," AIAA Paper 2000-2596, June 2000.

M. Sichel
Associate Editor